GRAPH SIGNAL PROCESSING OF HUMAN BRAIN IMAGING DATA

Weiyu Huang[*,†], *Thomas A. W. Bolton*[*,‡], *John D. Medaglia*[§,¶],
Danielle S. Bassett[‖,†], *Alejandro Ribeiro*[†], *and Dimitri Van De Ville*[‡]

ABSTRACT

Modern neuroimaging techniques offer disctinct views on brain structure and function. Data acquired using these techniques can be analyzed in terms of its network structure to identify organizing principles at the systems level. Graph representations are flexible frameworks where nodes are related to brain regions and edges to structural or functional links. Most research to date has focused on analyzing these graphs reflecting structure or function. Graph signal processing (GSP) is an emerging area of research where signals at the nodes are studied atop the underlying graph structure. Here, we review GSP tools for brain imaging data and discuss their potential to integrate brain structure with function. We discuss how brain activity can be meaningfully filtered. We also derive surrogate data as a null model to test significance for graph signals. We review that individuals with less concentration on graph high frequency could switch attention faster.

Index Terms— Brain, neuroimaging, network models, graph signal processing, functional MRI, structural MRI

1. INTRODUCTION

Advances in neuroimaging techniques such as magnetic resonance imaging (MRI) have provided opportunities to measure human brain structure and function in a non-invasive matter [2]. Diffusion-weighted MRI enables us to measure major fiber tracts in white matter and thereby map the structural scaffold that supports neural communication. Functional MRI (fMRI) takes an indirect measurement of the brain approximately each second, in the form of blood-oxygenation-level-dependent (BOLD) signals. An emerging theme in neuroimaging is to study the brain at the systems level with such fundamental questions as how it supports cognition, coordinated learning, and consciousness.

Connectomes, either structural or functional, have been effectively analyzed using a variety of tools from graph theory and network science [3]. These analyses have uncovered a variety of measures that reflect organizational principles of brain networks [4, 5]. Network analysis has also been applied to study behavioral, cognitive, and clinical measures either by statistical methods or machine learning tools [1, 6, 7].

Supported by ARO W911NF1710438, the Bertarelli Foundation, the Center for Biomedical Imaging (CIBM), NIH DP5-OD021352, the NIDCR R01-DC014960, the Perelman School of Medicine. [†]Department of Electrical and Systems Engineering, University of Pennsylvania. [‡]Institute of Bioengineering/Center for Neuroprosthetics, École Polytechnique Fédérale de Lausanne (EPFL). [§]Department of Psychology, Drexel University. [¶]Department of Psychology, University of Pennsylvania. [‖]Department of Bioengineering, University of Pennsylvania. The authors indicated with * contributed equally. Most results are adapted or reproduced with permission from [1]; see [1] for detailed discussion of implications for cognitive function.

As network neuroscience grows from understanding connectomes into understanding how connectomes and functional brain activity support behavior, the study of *dynamics* has emerged as central. To date, common approaches include examining changes in network structure [8] or investigating time-resolved measures of the underlying functional signals [9]. Since brain activity is mediated by physical connections, the network structure should be taken into account when examining these signals. Tools from the emerging field of graph signal processing (GSP) are tailored-made for this purpose.

In simple words, GSP addresses the problem of studying and extracting information from data defined not in regular domains, but on more irregular domains that can be conveniently represented by a graph. The fundamental GSP concepts that we utilize to analyze brain signals are the graph Fourier transform (GFT) and the corresponding notions of graph frequency components and graph filters. These concepts are generalizations of the Fourier transform, frequency components, and filters that have been used in regular domains such as time and spatial grids [10–12]. As such, they enable the decomposition of a graph signal into pieces that represent different levels of variability. We can define low graph frequency components denoting signals that change slowly with respect to brain networks in a well-defined sense, and high graph frequency components representing signals that change swiftly in a similar sense. This is important because low and high *temporal* variability have proven to be important in the analysis of neurological disease and behavior [13]. We review a recent study [1] that such a decomposition can be used to explain individual cognitive differences. The theory of GSP has been growing rapidly [7, 14–23].

2. BRAIN GRAPHS AND BRAIN SIGNALS

Brain networks describe physical connection patterns between brain regions. These connections are mathematically described by a weighted graph $\mathcal{G} := (\mathcal{V}, \mathbf{A})$ where $\mathcal{V}$ is a set of N nodes associated with brain regions and $\mathbf{A} \in \mathbb{R}^{N \times N}$ is a weighted adjacency matrix with entries $A_{i,j}$, each representing the strength of the link between brain regions i and j.

The brain regions encoded in the nodes of $\mathcal{V}$ are macro-scale parcels of the brain that our current understanding of neuroscience deems anatomically or functionally differentiated. There are various parcellations in use in the literature that differ mostly in their level of resolution [25]. As an example, the networks we study here consist of $N = 82$ regions; a schematic illustration of a few labeled brain regions is illustrated in Figure 1 (left).

The entries $A_{i,j}$ measure the strength of the axonal connection between region i and region j. This strength is a simple count of the number of streamlines that connect the regions, and

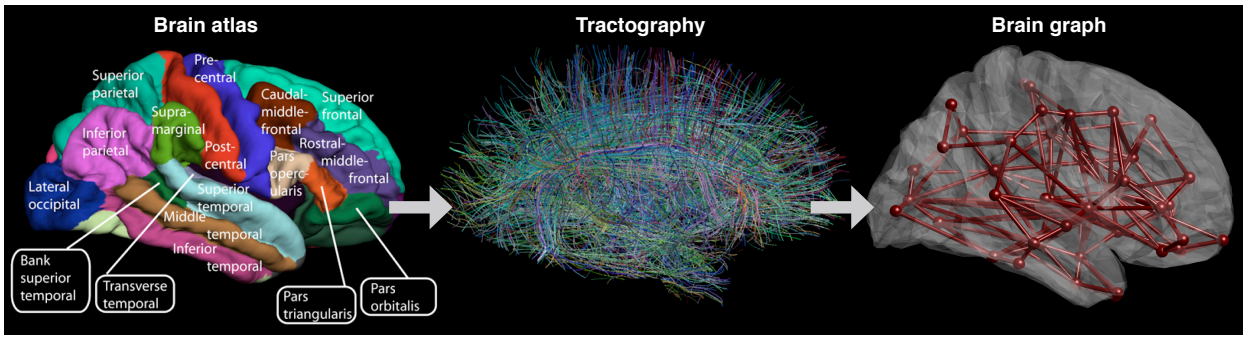

Fig. 1. **Example brain graphs**. Knowledge from an anatomical atlas according to anatomical features such as gyri and sulci (left) is combined with MRI structural connectivity extracted from diffusion-weighted MRI (middle), which can then be used to estimate the brain graph (right). [Adapted from [24]].

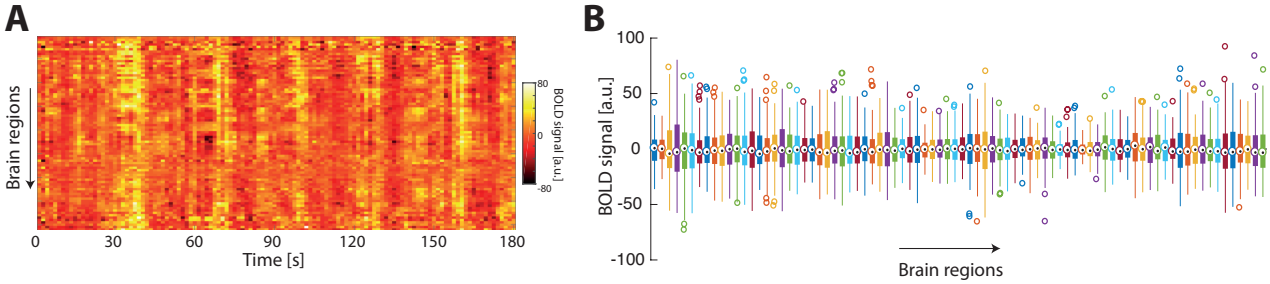

Fig. 2. **Example brain activity signals**. (**A**) For an example subject, the heat map of fMRI BOLD magnitude across brain regions (vertically) and time points (horizontally). (**B**) For the same subject, distribution of fMRI BOLD values for each brain region (horizontally) across all time points.

can be estimated with diffusion spectrum imaging (DSI) [26] — see Figure 1 for an illustration of the pipeline.

Besides structural connectivity, it is possible to also acquire brain activity signals $\mathbf{x} \in \mathbb{R}^N$ such that the value of the i-th component x_i expresses an indirect measure of neuronal activity in brain region i — see Figure 2 for an illustration of these BOLD signals. BOLD signals for all the N studied brain regions are measured over T successive time points, and therefore, we define the matrix $\mathbf{X} \in \mathbb{R}^{N \times T}$ such that its j-th column codifies brain activity at time j. An example of such a brain signal matrix is provided in Figure 2A, with the corresponding distribution of values for each brain region illustrated in Figure 2B.

Brain activity signals carry dynamic information that is not only beneficial for the study of pathology but also enables us to gain insight into human cognitive abilities. Whereas physical connectivity can be seen as a relatively stable property of individuals that changes slowly over the course of years, brain activity signals exhibit meaningful fluctuations at second or sub-second time scales that reflect how different parts of the brain exchange and process information in the absence of any external stimulus, and how they cooperate to meet cognitive challenges. There is increasing evidence that differences in activation patterns across individuals closely relate to behavioral variability [7, 27].

To the extent that brain activity signals are generated on top of the physical connectivity substrate, brain graphs and signals carry interdependent information and should be studied together. Here, we review the use of GSP tools for this purpose.

3. GSP FOR NEUROIMAGING

The GSP perspective is to interpret the brain signal $\mathbf{x}$ as a graph signal that is supported on the brain graph $\mathcal{G} = (\mathcal{V}, \mathbf{A})$. Here we review the fundamental operations that we will need for processing neuroimaging data in a meaningful way.

The focus of GSP is not on analyzing the brain graph $\mathcal{G}$ *per se*, but on using that graph to study brain signals $\mathbf{x}$. For a graph with positive edge weights, we consider a *graph shift operator* that captures the connectivity pattern of $\mathcal{G}$; we can choose the adjacency matrix $\mathbf{A}$ [10] or the graph Laplacian $\mathbf{L} = \mathbf{D} - \mathbf{A}$ [11], where the degree matrix $\mathbf{D}$ incorporates the degree of each node on its diagonal: $D_{i,i} = \sum_{j \in \mathcal{V}} A_{i,j}$. Let us denote the graph shift operator as $\mathbf{S}$ and assume henceforth that $\mathbf{S}$ is diagonalizable using singular value decomposition or Jordan decomposition, so that $\mathbf{S} = \mathbf{V}\mathbf{\Lambda}\mathbf{V}^{-1}$ where $\mathbf{\Lambda}$ is a diagonal matrix containing the eigenvalues $\lambda_k \in \mathbb{C}$, $k = 0, \ldots, N-1$, and $\mathbf{V} = [\mathbf{v}_0, \mathbf{v}_1, \ldots, \mathbf{v}_{N-1}]$. When $\mathbf{S}$ is symmetric we have that $\mathbf{V}$ is real and unitary, which implies $\mathbf{V}^{-1} = \mathbf{V}^\top$. The intuition behind examining $\mathbf{S}$ as an operator is to represent a transformation that characterizes exchanges between neighboring nodes. The eigendecomposition of $\mathbf{S}$ is used to define the graph spectrum.

Definition 1 *Consider a signal $\mathbf{x} \in \mathbb{R}^N$ and a graph shift operator $\mathbf{S} = \mathbf{V}\mathbf{\Lambda}\mathbf{V}^{-1} \in \mathbb{R}^{N \times N}$. Then, the vectors*

$$\tilde{\mathbf{x}} = \mathbf{V}^{-1}\mathbf{x} \quad \text{and} \quad \mathbf{x} = \mathbf{V}\tilde{\mathbf{x}} \tag{1}$$

form a Graph Fourier Transform (GFT) pair [10, 11].

The GFT encodes the notion of variability for graph signals akin to the one that the Fourier transform encodes for temporal signals [10]. Graph frequency ordering becomes more obvious for undirected graphs and thus symmetric adjacency matrices, as eigenvalues become real numbers. Specifically, the quadratic form of $\mathbf{A}$ is given by $\lambda_k = \mathbf{v}_k^\top \mathbf{A} \mathbf{v}_k = \sum_{i \neq j} A_{i,j} [\mathbf{v}_k]_i [\mathbf{v}_k]_j$. In this setup, lower frequencies will be associated to larger eigenvalues, to represent the fact that highly connected nodes in the graph possess signals with the same sign and similar values.

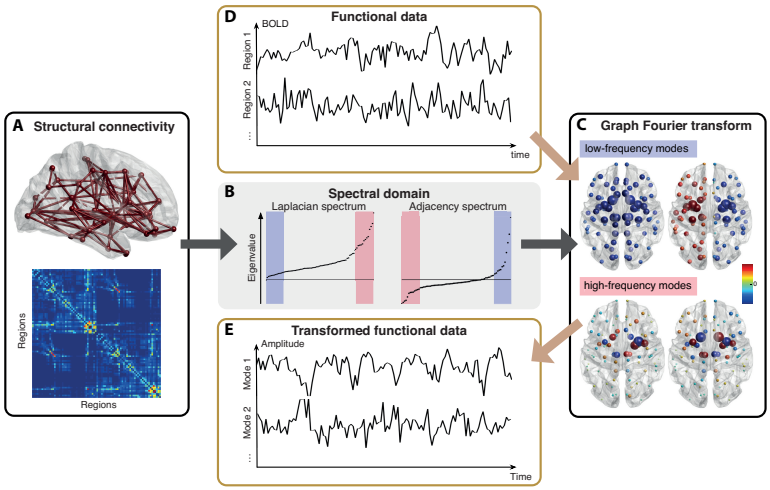

Fig. 3. **Graph signal processing for brain imaging**. (**A**) Structural connectivity from diffusion-weighted MRI, as seen in the form of a sagittal brain view (top) or of an adjacency matrix where the weights denote the strength of the connections (bottom), is used to construct a graph representing the brain's scaffold. (**B**) Through the eigendecomposition of the Laplacian (left plot) or adjacency (right plot) matrix, this structural graph can be examined in the spectral domain. The smallest Laplacian eigenvalues/most positive adjacency eigenvalues (labeled in blue) are associated to low-frequency modes on the graph (**C**, top brain views), while the largest Laplacian eigenvalues/most negative adjacency eigenvalues (denoted in red) relate to high-frequency modes (**C**, bottom brain views). These modes define the graph Fourier transform. Functional MRI data measured at the nodes of the graph (**D**) can be decomposed using these modes, and transformed using graph signal processing tools (**E**).

When using the graph Laplacian $\mathbf{L}$ as ashift operator [11] for an undirected graph, the quadratic form of $\mathbf{L}$ is given by $\lambda_k = \mathbf{v}_k^\top \mathbf{L} \mathbf{v}_k = \sum_{i \neq j} A_{i,j} ([\mathbf{v}_k]_i - [\mathbf{v}_k]_j)^2$. If the considered signal variations follow the graph structure, the resulting value will be low. Hence, in this setting, the eigenvectors associated to smaller eigenvalues can be regarded as the graph lowest frequencies.

Notice that the classical discrete Fourier transform (DFT) can also be obtained using the graph formalism by considering cycle graphs that represent discrete periodic signals [11]. For the undirected graph $\mathcal{G}$ with adjacency matrix $\mathbf{A}_{\text{cycle}}$ such that $[\mathbf{A}_{\text{cycle}}]_{i,i+1 \mod T} = [\mathbf{A}_{\text{cycle}}]_{i,i-1 \mod T} = 1$, and $[\mathbf{A}_{\text{cycle}}]_{i,j} = 0$ otherwise, the eigenvalues λ_k correspond to the squared DFT frequencies and the eigenvectors $\mathbf{v}_k$ of the Laplacian matrix $\mathbf{L}$ are equivalent to the DFT basis vectors.

Given the above relationships, it becomes possible to decompose the graph signals stored in the matrix $\mathbf{X}$ by extracting signal components associated to different graph frequency ranges. Specifically, we can define the diagonal filtering matrix $\mathbf{G}$, where $[\mathbf{G}]_{i,i} = g(\lambda_i)$ is the frequency response for the graph frequency associated with eigenvalue λ_i, and recover the filtered signals as:

$$\mathbf{Y}_{\mathbf{G}} = \mathbf{V}\mathbf{G}\mathbf{V}^\top \mathbf{X}. \tag{2}$$

Generic filtering operations can now be defined for the graph setting, such as ideal low-pass filtering, where $g(\lambda_i)$ would be 1 for λ_i corresponding to low-frequency modes, and 0 otherwise.

3.1. Generation of Graph Surrogate Signals

A pivotal aspect in any research field is to assess the significance of obtained results through statistical testing. More precisely, one aims at invalidating the so called *null hypothesis*. Non-parametric tests such as the permutation test provide a powerful alternative by mimicking the distribution of the empirical data. For correlated data, the Fourier phase-randomization procedure [28] has been widely applied as it preserves autocorrelation structure under stationarity assumptions. This standard method can be applied to the temporal dimension of our graph signals:

$$\mathbf{Y} = \mathbf{X}\mathbf{F}^H \mathbf{\Phi}_{\text{time}} \mathbf{F},$$

where the diagonal of $\mathbf{\Phi}_{\text{time}}$ contains random phase factors according to the windowing function $\Phi(\lambda_l) = \exp(j2\pi\phi_l)$, where ϕ_l are realizations of a random variable uniformly distributed in the interval $[0, 1]$. From the surrogate signals, one can then compute a test statistic and establish its distribution under the null hypothesis by repeating the randomization procedure.

The phase randomization procedure can be generalized to the graph setting by considering the GFT. In particular, the graph signal can be decomposed on the GFT basis and then the graph spectral coefficients can be randomized by flipping their signs. Assuming the random sign flips are stored on the diagonal of $\mathbf{\Phi}_{\text{graph}}$, we can formally write the procedure as

$$\mathbf{Y} = \mathbf{V}\mathbf{\Phi}_{\text{graph}}\mathbf{V}^\top \mathbf{X}. \tag{3}$$

For brain graphs, this procedure generates, for a given graph signal representing a measured activation pattern, surrogate graph signals that have the same smoothness measured on the graph.

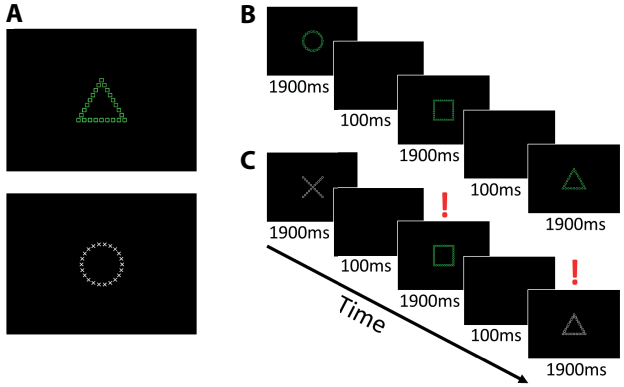

Fig. 4. **Cognitive task requiring perceptual switching**. (**A**) Example stimuli based on Navon local-global features. Subjects were trained to respond to the larger (or "global") shape if the stimulus was green and to the smaller (or "local") shapes if it was white. (**B**) An example of the non-switching condition. Subjects viewed a sequence of images and were instructed to respond as quickly and accurately as possible. (**C**) An example of the switching condition between stimuli requiring global and local responses. Here, trials with a red exclamation mark are switches from the previous stimulus.. [Reproduced with permission from [1]].

4. APPLICATIONS OF BRAIN GSP

We now discuss how the aforementioned GSP methods can be applied in the context of functional brain imaging. Figure 4 is adapted from [1]; Figures 5A and B are reproduced from [1]. For each volunteer, fMRI recordings were obtained when performing a Navon switching task, where local-global perception is assessed using classical Navon figures. Local-global stimuli were comprised of four shapes – a circle, cross, triangle, or square –

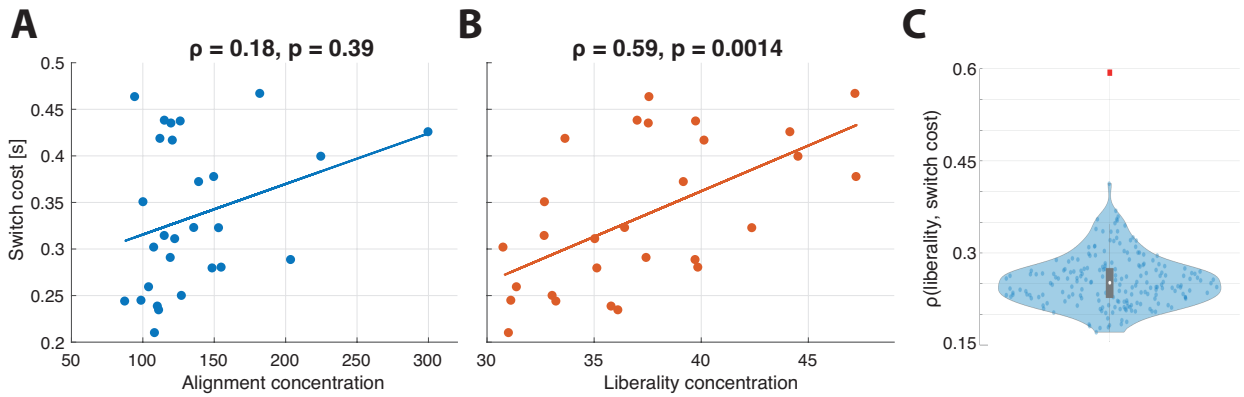

Fig. 5. **Switch cost correlates with the concentration in liberal signal**. (**A**) Switch cost does not significantly relate to the concentration of the graph low frequency components (alignment). (**B**) A lower concentration of graph high frequency components (liberality) is associated with a lower switch cost, that is, with faster attention switching. (**C**) The correlation between switch cost and liberal signal concentration is much stronger in the actual data than in null realizations for which statistical randomization has been performed in the graph domain. Blue data points denote the correlation coefficients obtained from surrogate signals under the null, while the red rectangle indicates the real correlation coefficient ($\rho = 0.59$). ρ, partial Pearson's correlation coefficient; p, p-value. [A and B are adapted with permission from [1]].

that were used to build the global and local aspects of the cues (see Figure 4A for indicative examples).

A response (button press) to the local shape was expected from the participants in the case of white stimuli, and to the global shape for green ones. Two different block types were considered in the experiment: in the first one (Figure 4B), the color of the presented stimuli was always the same, and the subjects thus responded consistently to the global or to the local shapes. In the second block type (Figure 4C), random color switches were included, so that slower responses were expected. The difference in response time between the two block types, which we refer to as *switch cost*, quantifies the behavioral ability of the subjects.

To study the brain correlates of attention switching, we decomposed the functional brain response into two separate components: one exhibiting *alignment* with structural connectivity (i.e., the regions that activate together are also physically wired), and one exhibiting *liberality* (jointly active areas possess high variability with respect to the underlying graph structure). To do so, we performed graph signal filtering as in (2) with two different filtering matrices: (i) $\mathbf{\Psi}_{\text{Al}}$, so that $\mathbf{Y}_{\mathbf{\Psi}_{\text{Al}}} = \mathbf{V}\mathbf{\Psi}_{\text{Al}}\mathbf{V}^{\top}\mathbf{X}$ is the transformed (low-pass filtered) functional data in which only the 10 lowest frequency modes are expressed at each time point; and (ii) $\mathbf{\Psi}_{\text{Lib}}$, for which $\mathbf{Y}_{\mathbf{\Psi}_{\text{Lib}}}$ only represents the temporal expression of the 10 largest frequency modes (high-pass filtering). At a given time point, the filtered functional signal varies in sign across brain regions; thus, to derive a subject-specific scalar quantifying alignment or liberality, we considered the norms of those signals as measures of concentration, which were eventually averaged across all temporal samples of a given subject.

To relate signal alignment and liberality to cognitive performance of the participants, we computed partial Pearson's correlation between our concentration measures and switch cost (median additional response time during switching task blocks compared to no-switching task blocks). Age and motion were included as covariates to remove their impact from the results. We observed a significant positive correlation between liberal signal concentration and switch cost ($\rho = 0.59$, $p < 0.0015$; see Figure 5B). Thus, the subjects possessing most liberality in their functional signals were also the ones for whom the attention switching task was the hardest. Regarding alignment, however, there was no significant association ($p > 0.35$; Figure 5A). In other words, the extent with which functional brain activity was in line with the underlying brain structural connectivity did not relate to cognitive abilities in the assessed task. From these results, one can see that a GFT framework enables one to isolate the functional components that are responsible for faster attention switching.

To more thoroughly examine the significance of the association between liberal signals and switch cost, we performed a null permutation test by generating graph surrogate signals as described in Sect. 3.1. Specifically, we generated 200 graph surrogate signals by randomly flipping the signs stored on the diagonal of $\mathbf{\Phi}_{\text{graph}}$, as in (3). Then, we evaluated the association between the null surrogate signals and switch cost. As seen in Figure 5C, the actual correlation coefficient between liberal signal concentration and switch cost (denoted by the red rectangle) is significantly larger than when computed on any of the null graph surrogate signals. This result indicates that the correlation between liberality and switch cost goes beyond what could be explained solely by structural connectivity.

In sum, we reviewed a recent study [1] that individuals whose most liberal fMRI signals were more aligned with white matter architecture could switch attention faster. I.e., relative alignment with anatomy is associated with greater cognitive flexibility. This observation complements prior studies of executive function that have focused on node-level, edge-level, and module-level features of brain networks [29]. This discussion illustrates the usefulness of GSP tools in extracting relevant cognitive features.

5. CONCLUSION

The GSP framework enables the analysis of brain activity on top of the structural brain graph. In particular, we have studied anatomically-aligned or -liberal organization of brain activity, and in the context of an attention switching task. We reviewed that concentration of signals liberal with anatomical connectivity is significantly correlated with higher cost in attention switching. These results reinforce the usage of GSP in brain signal analytics that were based on functional graphs [7]. Also, we used surrogate signal to generate graph null models to discuss that the significance of results cannot be explained by random permutation.

6. REFERENCES

[1] J. D. Medaglia *et al.*, "Functional alignment with anatomical networks is associated with cognitive flexibility," *Nat. Hum. Behav.*, vol. 2, no. 2, p. 156, Feb. 2018.

[2] M. Mather, J. T. Cacioppo, and N. Kanwisher, "Introduction to the special section: 20 years of fMRI-what has it done for understanding cognition?" *Perspect. Psychol. Sci.*, vol. 8, no. 1, pp. 41–43, Jan. 2013.

[3] M. Newman, *Networks: An Introduction*. New York, NY, USA: Oxford Univ. Press, 2010.

[4] E. Bullmore and O. Sporns, "Complex brain networks: graph theoretical analysis of structural and functional systems," *Nat. Rev. Neurosci.*, vol. 10, no. 3, pp. 186–198, Mar. 2009.

[5] O. Sporns and R. F. Betzel, "Modular brain networks," *Annu. Rev. Psychol.*, vol. 67, pp. 613–640, Jan. 2016.

[6] D. S. Bassett and M. G. Mattar, "A network neuroscience of human learning: Potential to inform quantitative theories of brain and behavior," *Trends Cogn. Sci. (Regul. Ed.)*, vol. 21, no. 4, pp. 250–264, Apr. 2017.

[7] W. Huang *et al.*, "Graph frequency analysis of brain signals," *IEEE J. Sel. Topic. Signal Process.*, vol. 10, no. 7, pp. 1189–1203, Oct. 2016.

[8] A. E. Sizemore and D. S. Bassett, "Dynamic graph metrics: Tutorial, toolbox, and tale," *NeuroImage*, in press.

[9] F. I. Karahanoglu and D. Van De Ville, "Dynamics of large-scale fMRI networks: Deconstruct brain activity to build better models of brain function," *Curr. Opin. Biom. Eng.*, vol. 3, pp. 28–36, Sep. 2017.

[10] A. Sandryhaila and J. M. Moura, "Discrete signal processing on graphs," *IEEE Trans. Signal Process.*, vol. 61, no. 7, pp. 1644–1656, Apr. 2013.

[11] D. Shuman *et al.*, "The emerging field of signal processing on graphs: Extending high-dimensional data analysis to networks and other irregular domains," *IEEE Signal Process. Mag.*, vol. 30, no. 3, pp. 83–98, May 2013.

[12] A. Ortega, P. Frossard, J. Kovačević, J. M. Moura, and P. Vandergheynst, "Graph signal processing," *arXiv preprint arXiv:1712.00468*, 2017.

[13] D. D. Garrett, N. Kovacevic, A. R. McIntosh, and C. L. Grady, "The modulation of BOLD variability between cognitive states varies by age and processing speed," *Cereb. Cortex*, vol. 23, no. 3, pp. 684–693, Mar. 2012.

[14] A. G. Marques, S. Segarra, G. Leus, and A. Ribeiro, "Sampling of graph signals with successive local aggregations," *IEEE Trans. Signal Process.*, vol. 64, no. 7, pp. 1832–1843, Apr. 2016.

[15] S. Chen, R. Varma, A. Sandryhaila, and J. Kovačević, "Discrete signal processing on graphs: Sampling theory," *IEEE Trans. Signal Process.*, vol. 63, no. 24, pp. 6510–6523, Dec. 2015.

[16] N. Perraudin, A. Loukas, F. Grassi, and P. Vandergheynst, "Towards stationary time-vertex signal processing," in *IEEE Int. Conf. Acoust., Speech, Signal Process.*, Mar. 2017, pp. 3914–3918.

[17] B. Pasdeloup, R. Alami, V. Gripon, and M. Rabbat, "Toward an uncertainty principle for weighted graphs," in *IEEE Euro. Signal Process. Conf.*, Aug. 2015, pp. 1496–1500.

[18] N. Tremblay and P. Borgnat, "Subgraph-based filterbanks for graph signals," *IEEE Trans. Signal Process.*, vol. 64, no. 15, pp. 3827–3840, Aug. 2016.

[19] R. Shafipour, A. Khodabakhsh, G. Mateos, and E. Nikolova, "A digraph Fourier transform with spread frequency components," *arXiv preprint arXiv:1705.10821*, 2017.

[20] R. Liu, H. Nejati, and N.-M. Cheung, "Simultaneous low-rank component and graph estimation for high-dimensional graph signals: application to brain imaging," *arXiv preprint arXiv:1609.08221*, Sep. 2016.

[21] Y. Wang, A. Ortega, D. Tian, and A. Vetro, "A graph-based joint bilateral approach for depth enhancement," in *IEEE Int. Conf. Acoust., Speech, Signal Process.*, May 2014, pp. 885–889.

[22] W. Huang, A. G. Marques, and A. Ribeiro, "Collaborative filtering via graph signal processing," in *IEEE Euro. Signal Process. Conf.*, Aug. 2017, pp. 1094–1098.

[23] E. Isufi, A. Loukas, A. Simonetto, and G. Leus, "Filtering random graph processes over random time-varying graphs," *IEEE Trans. Signal Process.*, vol. 65, no. 16, pp. 4406–4421, Aug. 2017.

[24] P. Hagmann *et al.*, "Mapping the structural core of human cerebral cortex," *PLoS Biol.*, vol. 6, no. 7, p. e159, Jul. 2008.

[25] A. Zalesky *et al.*, "Whole-brain anatomical networks: does the choice of nodes matter?" *Neuroimage*, vol. 50, no. 3, pp. 970–983, Apr. 2010.

[26] S. Gu, F. Pasqualetti *et al.*, "Controllability of structural brain networks," *Nat. Commun.*, vol. 6, p. 8414, Oct. 2015.

[27] D. S. Bassett *et al.*, "Dynamic reconfiguration of human brain networks during learning," *Proc. Natl. Acad. Sci. U.S.A.*, vol. 108, no. 18, pp. 7641–7646, May 2011.

[28] J. Theiler, S. Eubank, A. Longtin, B. Galdrikian, and J. Doyne Farmer, "Testing for nonlinearity in time series: the method of surrogate data," *Physica D*, vol. 58, no. 1, pp. 77–94, Sep. 1992.

[29] U. Braun *et al.*, "Dynamic reconfiguration of frontal brain networks during executive cognition in humans," *Proc. Natl. Acad. Sci. U.S.A.*, vol. 112, no. 37, pp. 11 678–11 683, Sep. 2015.